

Approved For Release STAT  
2009/08/26 :  
CIA-RDP88-00904R000100110

Dec

Approved For Release  
2009/08/26 :  
CIA-RDP88-00904R000100110



**Third United Nations  
International Conference  
on the Peaceful Uses  
of Atomic Energy**

▲/CONF.28/P/615  
UKRAINIAN SSR  
May 1964  
Original: RUSSIAN

Confidential until official release during Conference

PARAMETERS OF THE WWR-M REACTOR OF THE PHYSICS  
INSTITUTE OF THE UKRAINIAN ACADEMY OF SCIENCES AND  
ITS APPLICATION FOR THE NUCLEAR PHYSICS RESEARCH.

M.V.Pasechnik, I.F.Barchuk,  
V.P.Vertebny, M.F.Vlasov,  
V.V.Koloty, A.N.Maistrenko,  
V.I.Mostovoi, M.M.Nazarchuk,  
D.T.Pilipets, S.O.Slesarevsky.

Kiev, Ukr.SSR

Ukr.SSR Academy of Sciences, Institute  
of Physics.

I. Neutron Fluxes.

The 10 MW WWR-M research reactor of the Physics Institute of the Ukrainian Academy of Sciences /I/ has 9 radial horizontal channels, a thermal column and 13 vertical channels (Fig.Ia,Ib). At the nominal power level the average thermal neutron flux in the core is about  $10^{14} \text{ n/cm}^2 \text{ sec}$ . A number of works were carried out since the starting up of the reactor (II.I960). Some of them were devoted to the reactor parameters studies and others to the development of its assemblies and units.

The reactor neutron and  $\gamma$  -ray spectra were pub-

25 YEAR RE-REVIEW

lished earlier /3,4,5/.

For measurements of the relative distributions of thermal neutron fluxes in the reactor core and channels a copper indicator activation method was used. The measurement of the absolute value of the thermal neutron flux was made by the gold foils activation and measuring of their absolute activity by a  $\beta$ - $\gamma$  coincidence technique /6/.

So far as the experimental fast neutron spectrum of the reactor is known the absolute value of the fast neutron flux is easily obtained from the absolute activity of the threshold indicators.

In Fig. 2,3,4 the thermal and fast neutron flux distributions in the reactor channels are given for the core configuration, represented in Fig.5.

At the reactor power level 10MW the neutron fluxes are: in the centre of the core  $10^{14}\text{n/cm}^2\cdot\text{sec.}$ , in the centre of the water cavity  $3.2 \cdot 10^{14}\text{n/cm}^2\cdot\text{sec.}$ , at the horizontal channel outlet  $3.7 \cdot 10^9\text{n/cm}^2\cdot\text{sec.}$

## 2. The Increase of the WWR-M Reactor Power Level.

These studies were carried on the two directions: 1) the investigation of the fuel element temperature conditions in the core; 2) the development of sensitive methods of the fuel element leak control.

The thermal measurements were made to obtain:

- a) the temperature distribution of fuel element surface along the height and core radius;
- b) the effect of the control and safety rods upon this Distribution;
- c) the optimal choice of coolant flow rate for a given power level.

For these measurements a single fuel element was equipped by chromel-alumel thermocouples, situated on its surface, the diameter of the thermocouple wire being 0.05 - 0.1 mm.

In the first run the influence of the Be reflector

and control and safety rods on the surface temperature of the element located near the water cavity was studied. It appeared that the surface temperatures at the cavity side and at the core side do not appreciably differ. The closeness of control rods influences the surface temperature considerably. Curves 1 and 2 (Fig.6) show the surface temperature at the control rod side for cocked (curve 1) and inserted (curve 2) positions, and curves 3 and 4 show the same at the opposite side of the element for similar positions. In Fig.7 the radial core temperature distribution is represented. It is seen that the most thermally stressed core region is at its periphery near the Be reflector. For this region at a fixed flow rates of coolant the power level providing the temperature at the surface of full element equal to  $94-95^{\circ}\text{C}$  has been achieved. Fig.8 gives the temperature along the element height at 12 MW and flow rate  $1300 \text{ m}^3/\text{h}$ .

The above results can be summarized in the nomogram (Fig.9) that shows the ultimate power levels at the definite cooling conditions of the core. Along with this the element surface temperature (right-hand plot) and the cooling water temperature (left-hand plot) at the arbitrary power and flow rate are given.

At the reactor maintenance much attention was paid to the radiation security and elimination of environmental hazards. For this purpose a radiation area survey service was organized which systematically checks the natural  $\gamma$  - background of the fall-out, the activity of soil, vegetation and water both near the reactor and far from it. Any change in the reactor work conditions is always accompanied by the outer radiation control. Moreover, an effective leak control method for the fuel elements in the core was developed and regularly applied.

The element leak control was accomplished by a small ionization chamber into which the gaseous products of fission and radium emanation were pumped over from the large vacuum-chamber. The chamber volume ratio is 1:100. The diagram of the device is shown in Fig.10.

The scheme of the leak checking device is shown in Fig.10. For checking a fuel element is placed into the vacuum chamber, washed there, and then the chamber is vacuumed for half an hour. The gaseous products of fission and radium emanation which leak out of a damaged fuel element are supplented by distilled water from the vacuum chamber into ionization chamber the volume of the latter being one hundredth of the vacuum one.

When there is a leak the chamber gives a current, recorded on a chart.

### 3. The Nuclear Investigations.

The high neutron flux in the core, the possibility to vary the core configuration and the convenient reactor design allow for a wide range of experimental studies in different regions of science and engineering.

The investigations are made in nuclear physics, physics of condensed media, radiation material studies, chemistry and biology, according to the interests of the Academy of Sciences and other institutions of the Ukrainian SSR. The works on the last three subjects are published elsewhere /7,8/ and are not considered in this report. Here we consider only a few examples of nuclear investigations.

First of all we want to dwell upon the neutron spectrometry using the time-of-flight method. By this method the total and partial cross sections of the slow neutron interaction with nuclei are being measured. High flux reactor is particularly valuable for measurements of neutron cross sections of separated isotopes, available in small quantities. The measurements are made on the channel No.2, where the neutron beam is extracted directly from the core (Fig.16). This, in addition to the conical collimator system giving a convergent neutron beam, provides a maximum neutron flux in the resonance region. This channel is equipped by a single-slit neutron chopper with the 0.25 by 25 mm Slit.

The resolution of the chopper is  $0.2 \frac{\mu \text{sec}}{\text{m}}$  /9/.  
 Fig.18 shows the thermal neutron spectrum, measured at 12 MW with the Re I85 sample in the beam (slit 0.25 by 14 mm ).

The analysis of data obtained shows the possibility of measurements the neutron cross sections with beams of  $0.5 \text{ mm}^2$  or less by means of this technique.

Fig. 19 represents the results of the total neutron cross section measurements on separated isotopes of  $\text{Er}^{166}$ ,  $\text{Er}^{167}$ ,  $\text{Er}^{170}$  in the thermal region with resolution  $3 \frac{\mu \text{sec}}{\text{m}}$ . Fig. 20 shows similar cross sections in resonance region with resolution  $0.4 \frac{\mu \text{sec}}{\text{m}}$ .

The comparison of results obtained enables one to make an isotopic identification of levels and to determine their resonance parameters (Table I). The cross section of natural erbium at  $2200 \frac{\text{m}}{\text{sec}}$  is determined mainly by the  $\text{Er}^{167}$  isotope because of its two levels at 0.46 eV and 0.58 eV. As could be expected, the cross sections of even A erbium isotopes are much lower than that of  $\text{Er}^{167}$ . The magnitude of the total cross sections in the thermal region can hardly be explained with a help of the positive levels obtained early. It is possible that the large cross sections arise due to the negative levels, but, as no careful analysis was done the question is still open.

The investigations of total and partial neutron cross sections are also carried on at the channel No.9, where a 175-meter vacuum pipeline for neutron time-of-flight researches with three stations for detectors was built. The measurements can be made within the first 25 meters practically at any distance and also at distances 70, 125 and 175 meters. A set of mechanical choppers of different transmissions and resolutions is provided, allowing for measurements with resolution up to  $0.01 \frac{\text{sec}}{\text{m}}$  / 9,10 /.

In Fig.21 the cross section of natural phenium measured with  $0.05 \frac{\text{sec}}{\text{m}}$  resolution is represented. The isotope level identification was done from the single-

slit chopper measurements. At preset another mechanical chopper with diameter 500 mm is being installed at this channel /II/, having six divergent slits from 0.25 to 6 mm. This chopper will allow also to measure the total cross sections of separated isotopes available in small quantities with  $0.02 \frac{\mu\text{sec}}{\text{m}}$  resolution. The flight time measurements are made by means of IO24-Channel time analyzers with ferrite memory / I2 /.

In the first beam studies of differential cross sections of slow neutron inelastic scattering by the moderators on the thermal and epithermal regions are made by specialists of the Kurtchatov's Atomic Energy Institute. The monochromatic neutrons (resolution 0.2) are singled out by a mechanical monochromator with parabolic slits /Fig.22/. The scattered neutron spectra can be measured at angles  $15^\circ, 30^\circ, 60^\circ, 90^\circ$  and  $120^\circ$ . To increase the beam intensity the beam is extracted from the neutron flash-up in the berillium reflector. Moreover, to increase the neutron flux a water trap in the core near this channel was made. Fig.23 gives the spectrum of scattered neutrons at  $90^\circ$ .

The differential cross sections of slow monochromatic neutrons with energies 16; 46.6; 50.7; 102.3; 200 and 326 meV inelastically scattered on water and monoisopropyldiphenyl ( $\text{C}_{15}\text{H}_{16}$ ). From the cross sections obtained the average scattering characteristics  $E'(E)$ ,  $\frac{\gamma(E)}{\cos(\theta)}$ ,  $M_2$  and others were calculated. The comparison of cross sections and average characteristics of neutron scattering on water and monoisopropyldiphenyl shows that the chemical binding of hydrogen in monoisopropyldiphenyl is stronger than in water and the thermalization process of neutrons in monoisopropyldiphenyl is slower than in water.

The scattering law  $S(\alpha, \beta)$  and draw the generalized spectrum  $P(\beta)$  for  $\text{H}_2\text{O}$  at  $T=23^\circ\text{C}$  have been determined the data obtained can be used for neutron spectra calculations in the systems with water and organic moderators. More detailed description of the experiment and results is given in / I3 /.

The research program in the cold neutron region involves the investigations of total neutron cross sections as a function of energy and the dynamical structure of condensed phases studies with the help of inelastic scattering.

Fig. 25 shows the results of the measurements of total neutron cross sections of liquid oxygen and nitrogen in the 4-12 Å range, obtained by means of the neutron monochromator. One may notice a decrease of the cross section at 5.5 Å. This effect is similar to the cross section fall in crystals and can be attributed to the existence of the close order in liquids.

For studies in the cold neutron region a berillium filter cooled by the liquid nitrogen was designed. Also a simple mechanical slow neutron monochromator with longitudinal rotation axis and a simplified mechanical neutron chopper were built. The mechanical monochromator consists of two discs of 580 mm dia and 60 mm thick, spaced by 600 mm. The discs have 48 radial slits 2.7 mm wide and 80 mm height. As the collimator 40 mm wide has 17 slits, in any moment one of the slits is necessarily open. The monochromatization is accomplished by the incline of the shaft with respect to the neutron beam within 5°.

This effect especially manifests itself when the coherent diffraction prevails. It should be noted that the coherent diffraction cross sections are for oxygen 4.2 and for nitrogen 11 barns.

The increase of the cross section of the gases against the decrease of energy is supposed to be connected with unelastic scattering on rotational levels of nitrogen and oxygen molecules.

In liquid a cross section for unelastic interaction shows a deep fall. From this follows that in liquid the rotational movements are prohibited to great extent. Such investigations including temperature dependence will be of undoubted interest for gaseous condensation mechanism studies.

Table I

Levels and Neutron Cross-Sections of  
Erbium Isotopes.

Isotope	Energy of levels (ev)	$\Sigma$ (barns)	$g_{\text{neut}}$	Total cross section at the velocity 2200 m/sec in barns
I66	I5,9 $\pm$ 7 <sup>x)</sup>	(5 $\pm$ 0,5).10 <sup>3</sup>	0,003 $\pm$ 0,001	84 $\pm$ 10
	0,46 $\pm$ 0,012	-	-	
	0,584 $\pm$ 0,02	-	-	
I67	6,00 $\pm$ 0,17	(74 $\pm$ 8).10 <sup>3</sup>	0,015 $\pm$ 0,004	610 $\pm$ 16
	9,35 $\pm$ 0,34	(17 $\pm$ 3).10 <sup>3</sup>	0,005 $\pm$ 0,001	
	20,4 $\pm$ 1,1			
	27,1 $\pm$ 1,7 <sup>xx)</sup>	(33 $\pm$ 7).10 <sup>3</sup>	0,075 $\pm$ 0,010	
I68	+	-	-	37 $\pm$ 5
I70	98 $\pm$ 11			45 $\pm$ 6

x) In BNL-325 are given two levels in the region of I5 ev: I5,4 and I5,7 ev. If it is so, than we can state, that level I5,4 ev belongs to Er<sup>I66</sup>, because for natural erbium I5,4 ev level neutron width much more neutron width of the I5,7 ev level.

xx) The situation in this region is the same, as for I5 ev - case. Sowe can state, that 25,9 ev level, which is reported in BNL-235, belongs to Er-I67.

## LIST OF REFERENCES

1. Goncharov V.V. et al. Papers presented by the Soviet scientists at the Second International Conference on the Peaceful Uses of Atomic Energy, Vol. II, paper No. 2185.
2. M.V. Pasichnik, I.F. Barchuk, V.B. Klimontov. Experimental studies of the physical parameters of the VVR-M reactor of the physical institute of the Academy of Science of the Ukrainian SSR, published in the Ukrainian Physical Journal, Vol. VII, Nos. 1, 3, 1962.
3. M.V. Pasichnik, I.F. Barchuk, G.V. Belykh, V.P. Vertebnyi, et al. Gamma- and neutron spectra emitted by the horizontal channel of the VVR-M reactor of the physical institute of the Academy of Science of the Ukr. SSR. Preprint of physical institute, Academy of Science, Ukr. SSR., Kiev 1961.
4. Vertebny V.P., Vlassov M.F., Koloty V.V. et al. The neutron spectrum of the VVR-M reactor of the physical institute, Academy of Science, Ukr. SSR. 'Atomic Energy', Vol. V, No. 5, pg 324 (1962).
5. I.F. Barchuk, G.V. Belykh, V.I. Golyshkin, A.F. Ogorodnik. The gamma-spectrum of the VVR-M reactor of the physical institute, Academy of Science, Ukr. SSR. 'Atomic Energy', Vol. XII, No. 3, pg 251 (1962).
6. J.F. Raffle 'J. Nuclear Energy', 10, 8 (1958).
7. The biological effect of neutron irradiation. Collected works, Publ. House of the Academy of Sciences of the Ukr. SSR, Kiev 1964 (in print).  
 A.A. Gorodetsky, B.P. Kirichinsky, E.E. Chebotarev. On the relative biological effect of neutron irradiation. The Fourth Congress of Reprenologists and Health Physicists of the Ukr. SSR. Kharkov 1963 (Abstracts of papers)  
 B.P. Kirichinsky, E.E. Chebotarev. Changes in the average diameter of the erythrocyte under the influence of irradiation with fast neutrons. Fall session of the Biophysikalische Gesellschaft, Leibzig, 1963.  
 E.E. Chebotarev, B.P. Kirichinsky, I.M. Schuryan. On certain physico-chemical properties of blood under neutron irradiation. Abstracts of papers presented to the conference of the A.S. Popov Society, Kiev 1963.  
 B.P. Kirichensky, V.M. Pasichnik, Y.A. Tatsy, E.E. Chebotarev. On a method of irradiation of biological objects by fast neutrons. Abstracts of papers presented to the conference of the A.S. Popov Society, Kiev 1963.  
 Changes of Cl perfringens under the influence of nuclear irradiation. Microbiological Journal of the Academy of Science of the Ukr. SSR. Vol. XXV, No. 1, 10, 1963.  
 M.D. Matveeva. The effect of gamma- and neutron irradiations on the formation of toxins Cl perfringens of the 'a' type. In 'Genetics of micro organisms' Megiz, M. 1963, pg 219.  
 M.D. Matveeva. On a change in the formation of toxins of the bacteria Cl perfringens of the 'a' type effected by ionizing irradiations. In press, in a book "Biological effects of fast neutrons". Academy of Sciences of the Ukr. SSR.

- M.D. Matveev, M.S. Gornaya. The activity of alpha-toxin of radiation mutants *C1 perfringens* of the 'a' type.  
 Gornaya M.S., Pasichnik A.M. The effect of ionizing radiations on antigenic and umunagonic properties of the toxins of bacteria *C1. perfringens*. The first communication.  
 Resistance of the toxins, ionizing radiations on antigenic and umunagonic properties of the toxins of bacteria *C1. perfringens*.  
 Pasichnik A.M., Tulina G.G. Serological properties of radiation mutants of the bacteria *C1 perfringens*. The first communication. A study of the antigenic structure by a method of agglutinant absorption.  
 Balkasheva L.U., Palchevskaya A.E., Goncharenko S.V. The effect of fast neutrons on the morphological characteristics of the potato bacillus as culture.
8. Lavrentovich Y.I., Levon A.I., Kabakchi A.M. The effect of radiation of various magnitudes of linear energy transmission on polymeric films containing dyes. The Ukr. Chemical Journal 1964 (in press).
  9. Sokolovsky V.V. et al. Proceedings of the Second International Conference on the Peaceful Uses of Atomic Energy, papers presented by Soviet scientists, Vol. II, Atomisdat 59, pg 546, Section "Mechanical Selectors of the Atomic Energy Institute". M.F. Vlasov, V.P. Vetrebnny, A.Z. Kirilyuk. Identification and determination of the characteristics of erbium resonance levels. Ukr. Physical Journal, Vol. VIII, No. 9, pg 947.
  10. Vetrebnny V.P., Vlasov M.F., Koloty V.V., Maysterenko A.N., Ofengenden R.G., Pasichnik M.V., Pisanko Zh., I., Chzhu Yun-Tai. Investigations in the neutron spectrometry field carried out on the VVR-M atomic reactor. Proceedings of the Meeting on Slow Neutron Physics (7 - 12 December 1961) Dubna 1962.
  11. R.G. Ofengenden, G.S. Padun, N.M. Parovnik, G.B. Lyubansky. An analyser for simultaneous measurements of neutron spectra, background and effect, using a method of flight time. Proceedings of the 5th Conference on Nuclear Electronics. 1963.
  12. V.I. Mostovoy, I.P. Sadikov, A.A. Chernyshov, I.P. Ereemeev. A study of thermalizing properties of water and some other organic compounds by means of measurements of cross sections of inelastic scattering of slow monogramatic neutrons. I.V. Kurchatov Institute for Atomic Energy, Moscow 1963 (Preprint).

The List of Figures of the Report  
 "Parameters of the WWR-M Reactor of Physics Institute  
 of the Ukrainian Academy of Sciences and its Applica-  
 tion for the Nuclear Physics Research"

- Fig.1. a) Horizontal cross section of the reactor:  
 1. Control system channels  
 2. Technological section  
 3. Horizontal channel for experiments with  
     neutron beams  
 4. Be-reflector  
 5. Thermal column.  
 b) Vertical cross section of the reactor:  
 1. Water entrance  
 2. Water excite  
 3. Horizontal channel for experiments with  
     neutron beams.  
 4. The reactor vessel  
 5. Thermal column.
- Fig.2. Radial (the neutron beam hole No.2) and height (chan-  
 nels 42/60 and 62/60) neutron flux distribution in  
 the reactor.
- Fig.3. Absolute values of the thermal and fast ( $E_n \geq 1 \text{ M ev}$ )  
 neutrons in the channels 75/60; 63/60; 62/60; 7/60;  
 95/60.
- Fig.4. Absolute values of the thermal and fast neutrons in  
 the channels 36/60; 42/60; 46/60:
- Fig.5. The configuration of the core of the reactor.
- Fig.6. The Influence of the control rod on the temperature  
 of the fuel rod wall.
- Fig.7. Fuel rods temperature distribution vs the core radius.
- Fig.8. Fuel rod temperature distribution vs the core height.
- Fig.9. The conditions of the reactor cooling at different  
 power levels.

Fig.I0. A Scheme of the system:

1 - evacuated chamber, 2 - ionization chamber,  
3 - filter, 4 - for vacuum ballon, 5 - for vacuum  
pump, 6 - water level indicator, 7 - vessel for  
distillated water, 8 - self-recorder of ionization  
current, 9 - self-recorder of fuel-rod temperature.

Fig.II. Scheme of the Experiment on the neutron cross section  
of separated isotopes:

- I. The reactor core
2. The reactor schield
3. Collimators
4. The neutron chopper
- 5,6. Boron-hydrogen shield at the chopper excite
7. Chopper Shield
8. Vacuum evacuated tube
9. Detector station shield
10.  $B^{10}F_3$  - detector
- II. Boron shield of the detector
12. Neutron trap.

Fig.I2. Experimental thermal neutron spectrum with the sam-  
ple  $Re^{185}$  ( area of the neutron beam  $0,25 \times 10 \text{ mm}^2$  )  
on  $\gamma$  -axis-intensity in thousand counts per chan-  
nel per hour, on X -axis-time of flight. One chan-  
nel -  $3,4 \frac{\mu\text{sec}}{m}$  . Power level of the reactor -  
 $12 \text{ Mwt. n} - 3,39 \cdot 10^{21} \frac{\text{nuclei}}{\text{cm}^2}$  .

Fig.I3. The total thermal neutron cross sections of the  
isotopes of Erbium (resolution  $3,4 \frac{\mu\text{sec}}{m}$  ).

Fig.I4. The total resonance neutro n cross section of the  
Erbium isotopes (resolution  $0,4 \frac{\mu\text{sec}}{m}$  ).

Fig.I5. Natural rhenium transmission vs neutron time of  
flight. Levels indentification has been made by  
means one-slit chopper.

Energy lãvels 2,156; 5,93; 7,18; 11,94; 12, 90;  
14,74; 21,46; 34,08(?) and 41,50 ev are ones of  
 $Re^{185}$ .

Energy levels 4,41; 11,20; 16,16; 17,69; 18,53;  
32,57(?) and 39,60 ev are ones of  $Re^{187}$ .

The Sample Thickness  $4,537 \text{ gr/cm}^2$ .

Fig.I6. The Experiment on measurements of angular distributions of the inelastic scattered neutrons in slowing-down media.

Fig.I7. A - Spectrum of scattered neutron by  $\text{H}_2\text{O}$  at  $90^\circ$ ; incident neutron energy  $111,5 \cdot 10^{-3} \text{ ev}$ .

Fig.I8. Total neutron scattering cross section of liquid nitrogen at the  $77^\circ\text{K}$  vs neutron wave length. Upper curve - total scattering cross section of  $\text{N}_2$ -gas (given for comparison). Measurements with liquid nitrogen has been made with the chopper and the monochromator.

Fig.I9. Total cross section of liquid oxygen at boiling temperature vs neutron wave length. Upper curve - data for gas (BNL-325).

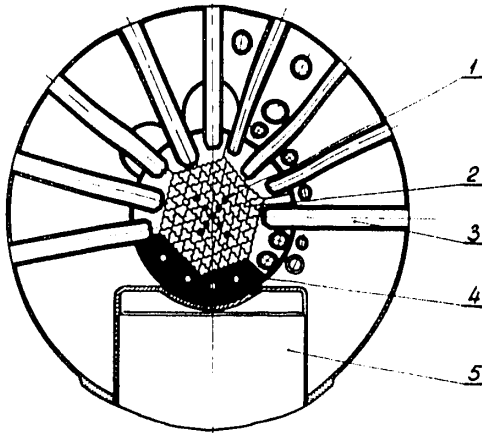


Fig. 1a

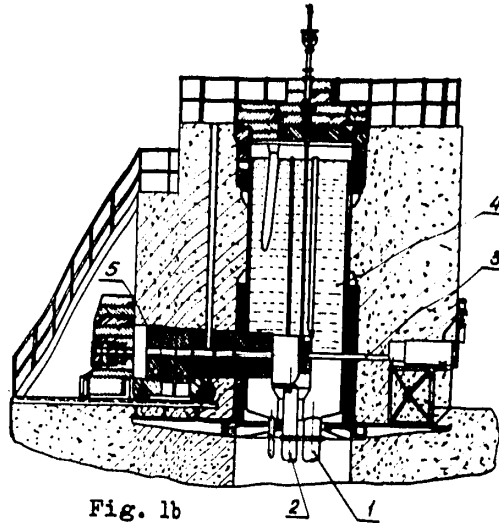


Fig. 1b

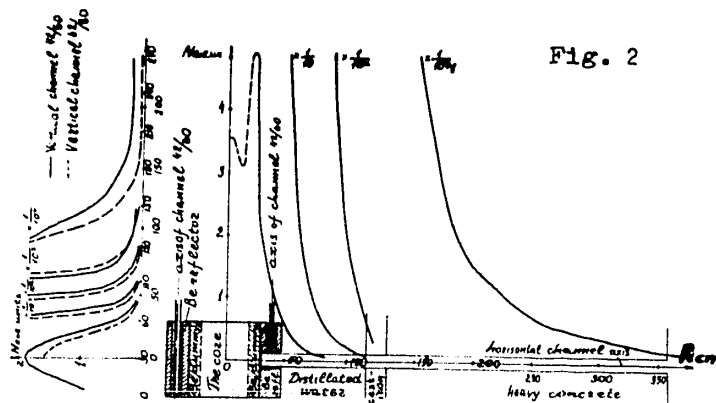


Fig. 2

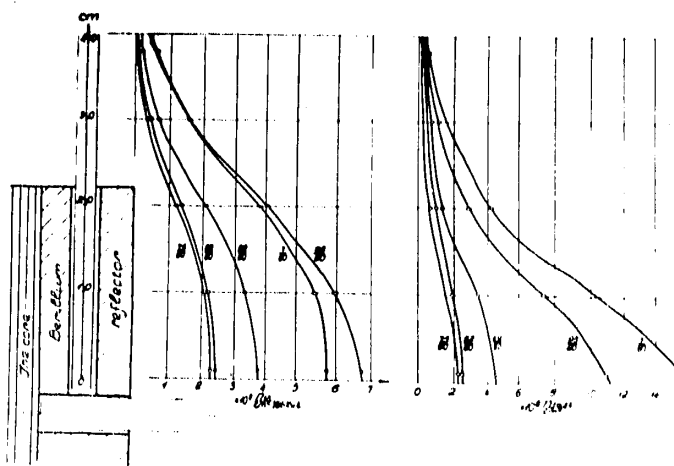


Fig. 3

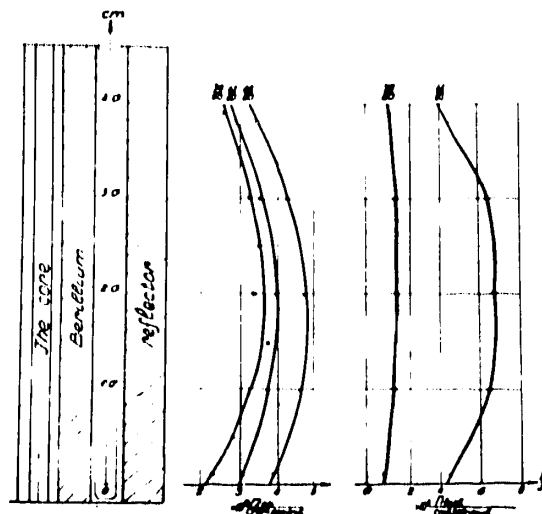


Fig. 4

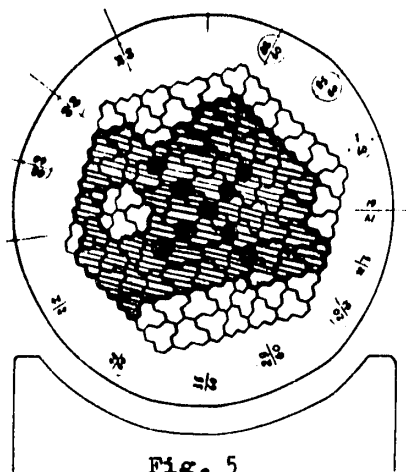


Fig. 5

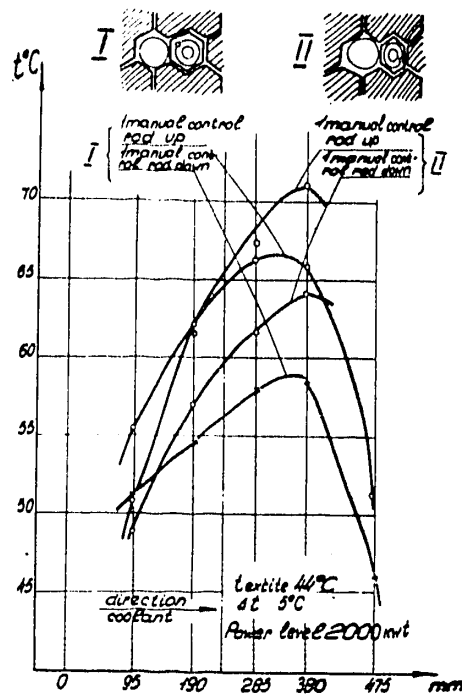


Fig. 6

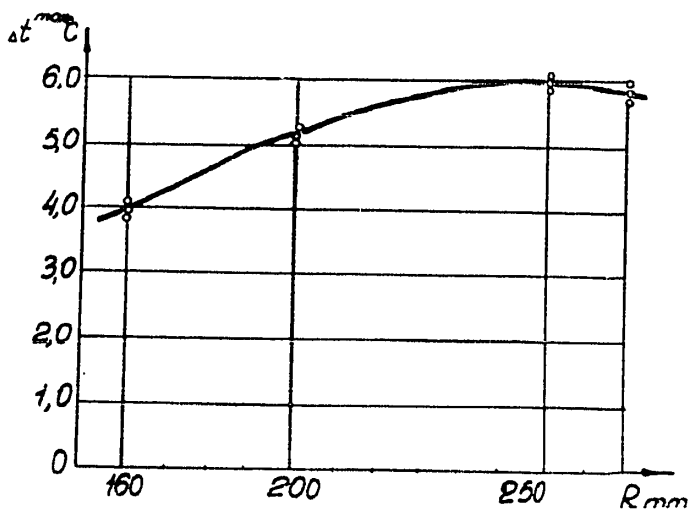
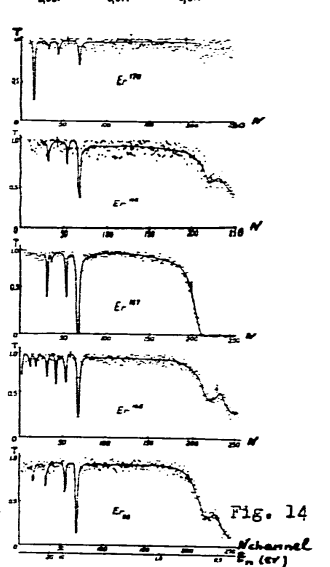
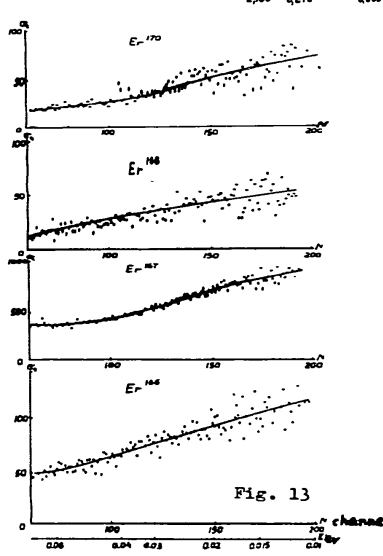
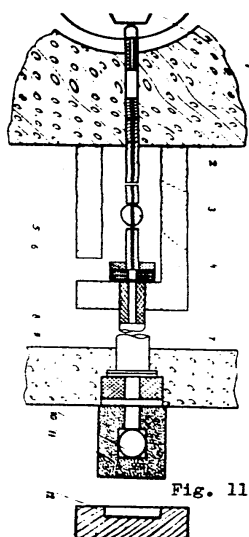
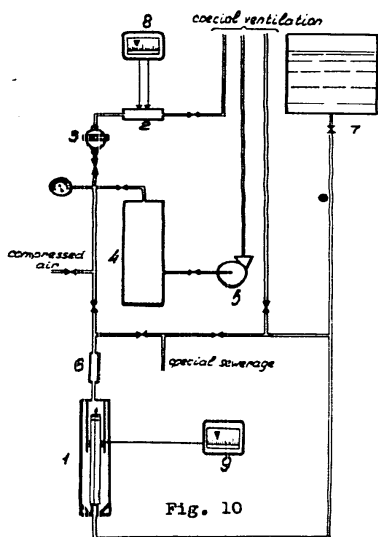
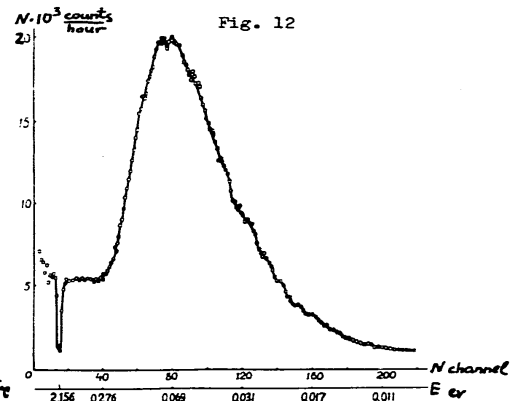
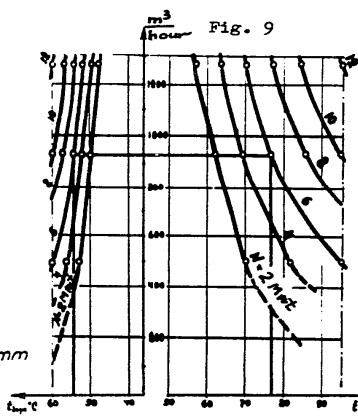
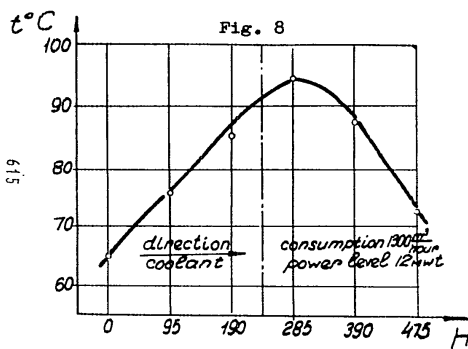


Fig. 7

615



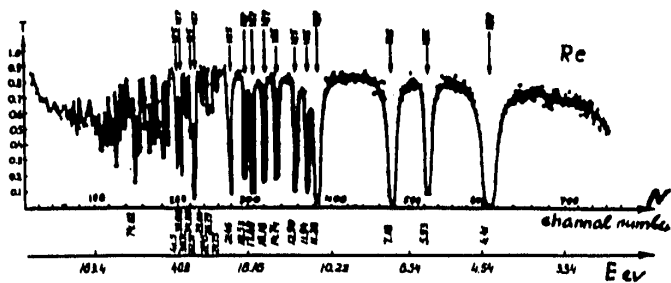


Fig. 15

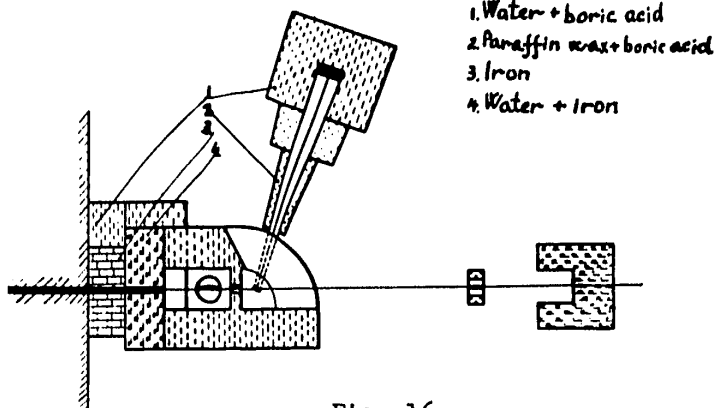


Fig. 16

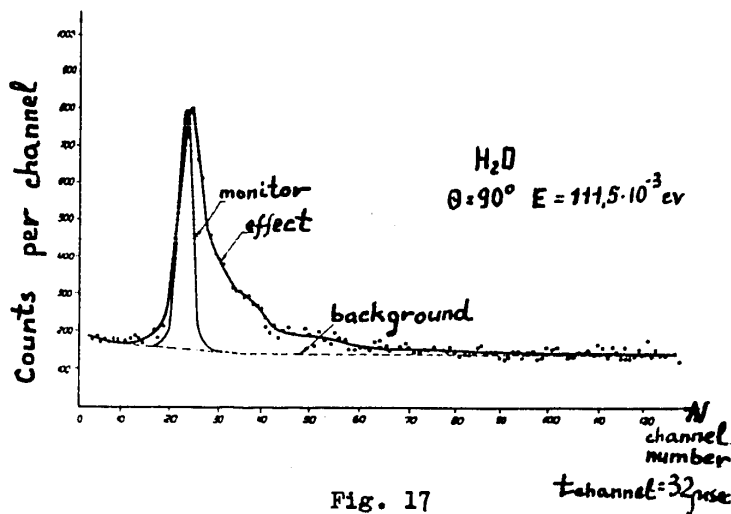


Fig. 17

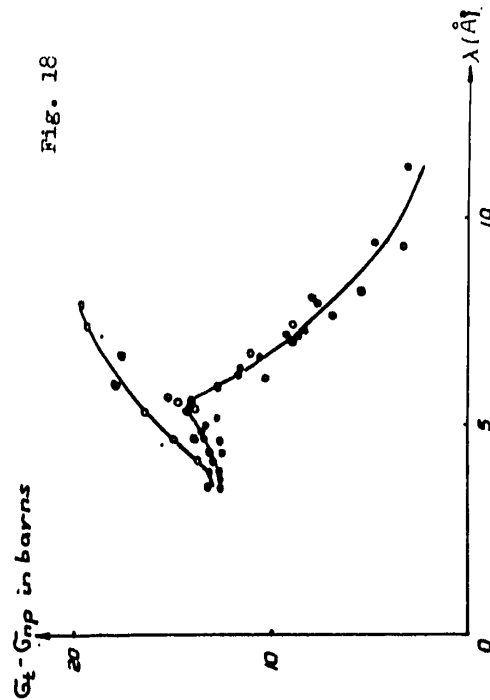


Fig. 18

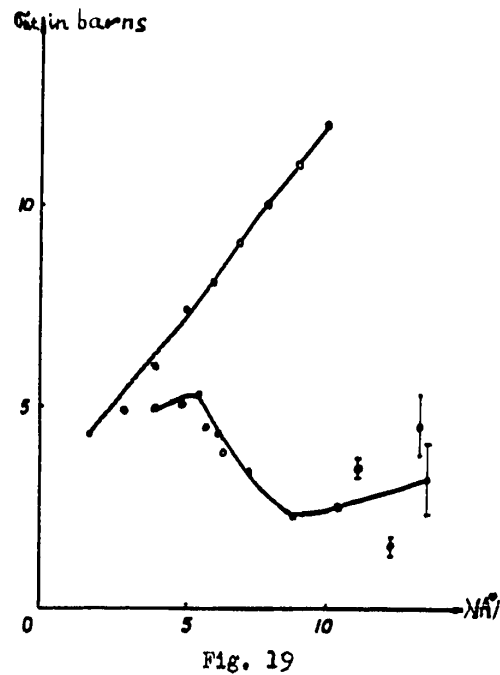


Fig. 19